

Compton Scattering by *K*-Shell Electrons

J. W. MOTZ* AND G. MISSONI

Laboratori di Fisica, Istituto Superiore di Sanità, Rome, Italy

(Received May 23, 1961)

The differential cross section $d\sigma_K$, for the Compton scattering of 660-kev photons by the *K*-shell electrons of tin and gold, is determined by an experimental method in which a scattered photon is selected in coincidence with an accompanying *K* x ray. This cross section is compared with the Klein-Nishina cross section $d\sigma_F$ for an electron *initially free and at rest*. The results show that the ratio $d\sigma_K/d\sigma_F$ approaches zero as the photon scattering angle decreases to zero. This behavior agrees qualitatively with the small angle behavior predicted by exact nonrelativistic calculations for the hydrogen atom. For large angles, this ratio is greater than unity and at 110 degrees is equal to approximately 1.2 for tin and 1.4 for gold. The experimental values for $d\sigma_K$ at large angles agree with the theoretical values for the Compton cross section (averaged over the angle between the incident photon and electron) for electrons *initially free but with velocities corresponding to the *K*-shell binding energy*. Also, the results indicate that the small- and large-angle behavior for $d\sigma_K$ has a compensating effect in which the ratio of the total cross sections σ_K/σ_F (integrated over the photon scattering angle) is approximately equal to unity for both tin and gold.

1. INTRODUCTION

THE Compton process generally refers to the case in which a photon is scattered by an electron initially at rest and free to the extent that the atomic binding energy is negligible compared to the energy acquired from the photon. Under these conditions, the quantitative behavior¹ of the process is relatively well established. The kinematics for the process are derived from the usual conservation laws and the cross section is predicted with good accuracy by the Klein-Nishina formula.¹

On the other hand, the process becomes more complicated for the case where the binding energy of the electron cannot be neglected. The bound electron forces the atom to participate in the process and there is a certain probability that energy will be transferred to the atom. In the present discussion, the Compton process for the bound electron refers only to the *incoherent* scattering process in which the atom absorbs energy. A comparison of the Compton process for a free electron and for a bound electron can be expected to reveal two important differences: (1) the energies of the photons scattered at a particular angle by bound electrons are not uniquely determined, but have a certain distribution extending from zero to $k_0 - I$, where k_0 is the incident photon energy and I is the binding energy of the electron, and (2) the differential Compton cross section at small angles is less for a bound electron than for a free electron. At present very few quantitative studies of these differences are available.

Most of the present information on the Compton process for bound electrons pertains to the energy

distribution (width of the Compton-shifted line) of the photon scattered at large angles (≥ 90 degrees) by *all* of the electrons in an atom. This information was provided principally by DuMond and his collaborators.² Their studies were carried out in the nonrelativistic region ($k_0 \ll m_0 c^2$) for atoms with low atomic numbers ($Z \leq 6$). Under these conditions the initial photon energy is small compared to the electron rest energy, the energy transferred in the collision is small compared to the initial photon energy, and the atomic binding energies are less than the energy transferred in a free electron collision. The main results obtained in these investigations were as follows: (1) The energy distribution of the Compton line was shown to correspond to the Doppler broadening produced by electrons having a given momentum distribution prescribed for electrons in the atom; (2) the energy width of the line at half-intensity was estimated to be approximately equal to $4[I(k_0 - k)]^{1/2}$, where I is the binding energy of the electron and k_0 and k are the initial and final photon energies, respectively, for scattering by free electrons; and (3) the most probable photon energy for incoherent scattering by bound electrons at large angles is greater than the photon energy for scattering by free electrons by an amount of the order of $k^2 I / (k_0^2 - kI)$.

Information¹ on the Compton cross section for bound electrons has been obtained mainly from nonrelativistic calculations. These calculations give estimates of a correction factor for the Klein-Nishina formula evaluated for all of the atomic electrons of a given element. This correction factor is expressed in terms of an incoherent scattering function which gives the probability that an atom will absorb energy and be raised to an excited or ionized state when an incident photon transfers momentum to any of the atomic electrons. Different nonrelativistic atomic models have been used

* On assignment from the National Bureau of Standards, Washington, D. C., September 1960-1961.

¹ An extensive review of this behavior has been given by Robley D. Evans, *Encyclopedia of Physics* (Springer-Verlag, Berlin, 1958), p. 218. Also a summary of detailed data about the Compton process has been prepared by Ann T. Nelms, National Bureau of Standards Circular No. 542 (U. S. Government Printing Office, Washington, D. C., 1953).

² J. W. M. DuMond, *Revs. Modern Phys.* **5**, 1 (1933); J. W. M. DuMond and P. Kirkpatrick, *Phys. Rev.* **52**, 419 (1937) and **54**, 802 (1938); F. Bloch, *ibid.* **46**, 674 (1934); E. Ross and P. Kirkpatrick, *ibid.* **46**, 668 (1934).

TABLE I. Summary of coincidence data.

Scattering angle θ (degrees)	Target-crystal distance (inches)		Z	Target		Total T $\times 10^3$	Coincidence counting rate (seconds ⁻¹)		
	γ detector	K detector		Thick-ness (mg/cm ²)	Inclination angle, α (degrees)		Chance C $\times 10^3$	False F $\times 10^3$	$(=T-C-F)$ $\times 10^3$
20	5.3	0.75	50	7.5	0	15.0 ± 0.3	1.69 ± 0.10	8.57 ± 0.39	4.70 ± 0.50
			79	6.7	60	17.0 ± 0.4	5.81 ± 0.20	7.42 ± 0.54	3.81 ± 0.70
30	5.1	0.75	50	7.5	0	14.3 ± 0.3	1.12 ± 0.09	7.90 ± 0.55	5.23 ± 0.63
40	4.0	0.75	50	7.5	0	27.9 ± 0.5	1.12 ± 0.10	16.9 ± 0.8	9.83 ± 1.00
			79	6.7	60	31.9 ± 0.7	5.30 ± 0.26	18.4 ± 0.7	8.20 ± 1.00
60	3.0	1.75	50	7.5	0	7.90 ± 0.19	0.458 ± 0.047	4.54 ± 0.29	2.90 ± 0.35
			79	6.7	60	10.7 ± 0.2	2.24 ± 0.11	5.00 ± 0.34	3.40 ± 0.41
110	3.7	1.75	50	7.5	0	2.54 ± 0.09	0.530 ± 0.040	0.755 ± 0.100	1.26 ± 0.14
			79	6.7	60	4.73 ± 0.14	2.44 ± 0.08	0.550 ± 0.055	1.80 ± 0.17

to estimate this incoherent scattering function.³ The general behavior of this function is that it approaches zero or unity depending on whether the momentum transfer to the atomic electron is small or large, respectively, compared to the initial electron momentum. It should be emphasized that the cross-section formula obtained from these calculations is a function of the photon scattering angle and is integrated over all photon energies⁴ at a given angle. Also this cross section applies to photon scattering from all of the atomic electrons, which can have different binding energies. In addition to these nonrelativistic calculations,³ an experimental investigation of the Compton cross section for bound electrons has been reported by Brini *et al.*,^{5,5a} with the result that the cross section for the Compton scattering of 660-keV photons by the *K*-shell electrons of lead is roughly an order of magnitude larger than the cross section for scattering by free electrons.

The present work was undertaken to provide more data on the Compton cross section for bound electrons, and was prompted by the fact that the above experimental study by Brini *et al.*⁵ did not account for false events which are of paramount importance in the determination of any meaningful data (see Secs. 2B, 2E, and Table I). In the present measurements the cross section for the Compton scattering of 660-keV photons from the *K*-shell electrons of tin ($Z=50$) and gold

($Z=79$) is investigated as a function of the photon scattering angle (from 20 to 110 degrees). The selection of only *K*-shell electrons in the scattering process permits a study of the cross section as a function of the atomic binding energy. The atomic binding effects are most important for the *K*-shell electrons, and in these measurements the *K*-shell binding energies of the high- Z targets are relativistic and are comparable to the incident photon energy.

2. EXPERIMENTAL PROCEDURE

A. Method and Arrangement

The incoherent scattering of a photon by a *K*-shell electron requires the ejection⁶ of the electron from the *K* shell. Therefore, there is a certain probability that this type of scattering will be accompanied by the emission of a *K* x ray. The above condition is used to distinguish between the photons scattered incoherently by the *K*-shell electrons and the photons scattered by the free (or more loosely bound) electrons. In the present measurements, the apparatus is designed to select events in which the scattered photon is emitted in coincidence with a *K* x ray.

The experimental arrangement for these measurements is shown in Fig. 1. Photons with an energy of approximately 660 keV are emitted from a 10-curie radioactive source of Cs¹³⁷, and pass through a collimator to the target. For the *K*-shell scattering there are two different targets: a 6.7-mg/cm² gold foil with the angle of inclination, α , equal to 60 degrees and a 7.5-mg/cm² tin foil with α equal to zero degrees (see Fig. 1 and Sec. 2E). The scattered photons are detected by a scintillation spectrometer (γ -detector in Fig. 1) with a $\frac{3}{4}$ -in. diam lead collimator and a 1-in. diam, 1-in. thick NaI(Tl) crystal. The 0.3-g/cm² aluminum window of the γ -detector crystal stops the electrons scattered from the target and from the edges of the collimator. (For scattering angles less than 60 degrees the aluminum window thickness was increased to 0.6-g/cm².) Measurements were made for values of the scattering angle, θ , equal to 20, 30, 40, 60, and 110 degrees. The *K* x rays emitted from the target are detected by a second

³ A survey of the various theoretical results that have been obtained for the incoherent scattering function has been prepared by Gladys White Grodstein, National Bureau of Standards Circular No. 583 (U. S. Government Printing Office, Washington, D. C., 1957), p. 51.

⁴ An example of a cross-section calculation that is integrated only over a small interval of photon energies has been given by J. Randles, Proc. Phys. Soc. (London) **70**, 337 (1957). This calculation is intended to estimate the correction due to incoherent scattering effects in coherent scattering measurements, and only applies to photons scattered incoherently at large angles from bound electrons in a small energy interval near the upper limit.

⁵ D. Brini, E. Fuschini, N. T. Grimellini, and D. S. R. Murty, Nuovo cimento **16**, 727 (1960).

^{5a} Note added in proof. We have been informed that a similar study for the *K* electrons of lead has been reported recently by Z. Sujkowski and B. Nagel [Arkiv Fys. **20**, 323 (1961)]. For small angles ($<90^\circ$), their results for the cross section ratio $d\sigma_K/d\sigma_F$ are qualitatively similar to the present results for the *K* electrons of tin and gold. For large angles where the momentum transfer to the electron is large compared to its initial momentum, their data is not sufficient to confirm the present results that this cross section ratio is larger than unity and increases with the average velocity (or binding energy) of the *K* electron.

⁶ If the electron is not removed from the *K* shell as a result of the momentum transfer from the incident photon, the atom does not absorb any energy and the scattering process is coherent.

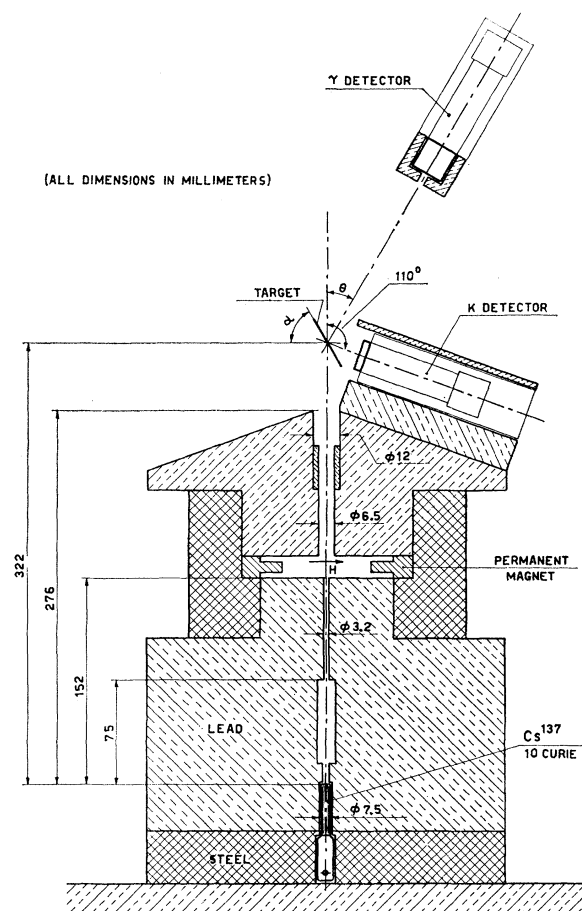


FIG. 1. Experimental arrangement. The γ detector and the K detector are two scintillation spectrometers with a 1-in. diam, 1-in. thick NaI(Tl) crystal (behind a $\frac{3}{4}$ -in. diam lead collimator) and a 1-in. diam, $\frac{1}{4}$ -in. thick NaI(Tl) crystal, respectively. Distances between the target and the detectors are given in Table I. The angle of the target inclination, α , is 60 degrees for the 6.7-mg/cm² gold target and zero degree for the 7.5-mg/cm² tin target. Values of the scattering angle, θ , are equal to 20, 30, 40, 60, and 110 degrees. The permanent magnet in the collimator is used to reduce the number of electrons scattered in the direction of the target.

scintillation spectrometer (K detector in Fig. 1) with a 1-in. diam, $\frac{1}{4}$ -in. thick NaI(Tl) crystal, which is positioned with its axis at an angle of 110 degrees with respect to the direction of the incident photon beam. The K -detector crystal is covered with a 0.013-g/cm² beryllium window for the tin target measurements and an additional 0.27-g/cm² aluminum foil (to absorb the L x rays) for the gold target measurements (see Fig. 3). The distances between the target and the detector for the different scattering angles are given in Table I.

The pulses from each detector in Fig. 1 pass to an amplifier, a single-channel pulse-height selector with a window width that can be varied from zero to 100 v, and a coincidence analyzer with a resolving time of approximately 5×10^{-7} sec. This resolving time was found to be large enough to accommodate the inherent time spread between the pulses with the minimum and

maximum heights accepted by the window of the pulse-height selector. Samples of the pulse height distributions for each detector were obtained with a 200-channel pulse-height analyzer, and are shown in Figs. 2 and 3.

The pulse height distributions for the γ detector are given in Fig. 2. These distributions were measured with 0.22-g/cm² aluminum target for values of θ equal to 20, 40, 60, and 90 degrees. The photon energies corresponding to these values of θ for Compton scattering from the electrons initially free and at rest are equal to 612, 508, 402, and 288 kev, respectively. For all angles in the coincidence measurements, the window of the pulse height selector for the γ detector accepts pulses with minimum and maximum amplitudes corresponding to the values at the peak intensity of the photopeak curves produced by photons with energies approximately equal to 100 and 750 kev, respectively.

The pulse height distributions for the K detector are given in Fig. 3. These distributions are produced by the K x rays (≈ 25 kev)⁷ emitted from a tin target [Fig. 3(a)] and by the K x rays (≈ 70 kev)⁷ and L x rays

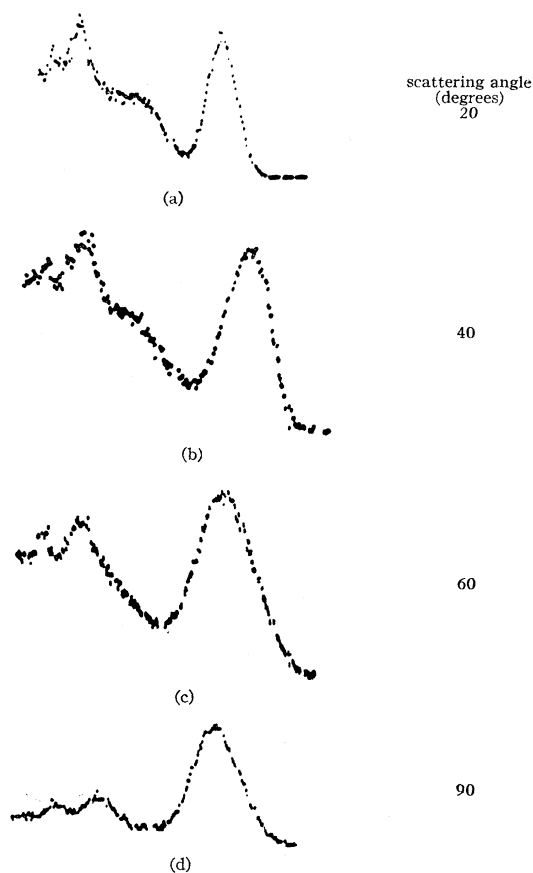


FIG. 2. Pulse height distributions of the γ detector measured with a 200-channel pulse height analyzer and with a 0.27-g/cm² aluminum target. The approximate photon energies corresponding to the different scattering angles are 610 kev for 20 degrees, 510 kev for 40 deg, 400 kev for 60 degrees, and 290 kev for 90 degrees.

⁷ S. Fine and C. F. Hendee, *Nucleonics* **13**, 36 (1955).

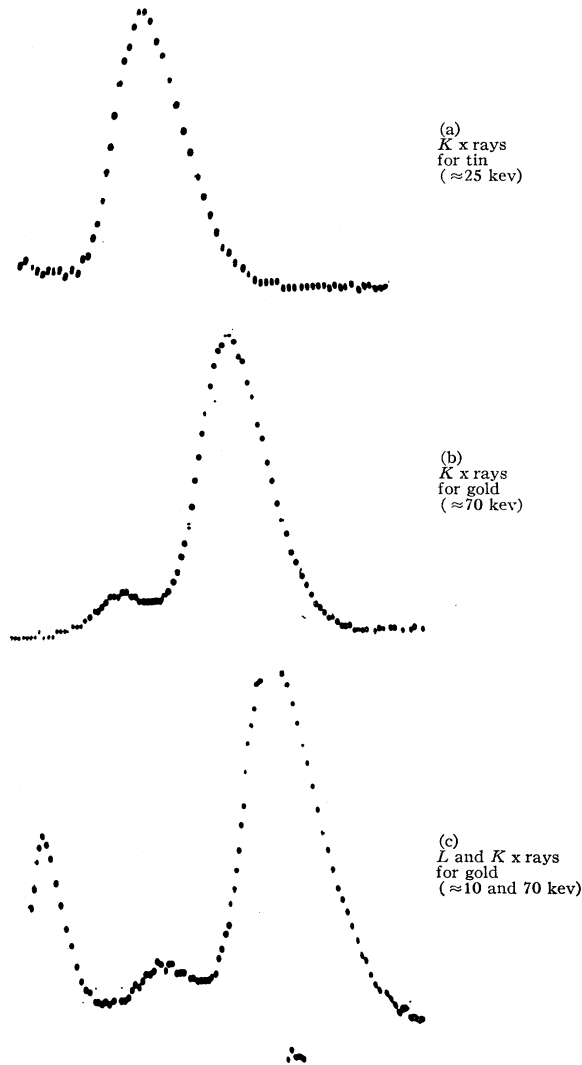


FIG. 3. Pulse height distributions of the K detector measured with a 200-channel pulse-height analyzer. These curves represent the difference in the distributions obtained (a) with a tin target and with an equivalent aluminum target (having the same number of electrons per cm^2), (b) with a gold target and with an equivalent aluminum target, plus a 1-mm aluminum absorber over the K -detector window, and (c) with the same targets as (b) but without the 1-mm aluminum absorber.

(≈ 10 keV)⁷ emitted from a gold target [Fig. 3(b) and (c)]. The distribution (b) for the K x rays from gold shows a second small peak produced by the escape of the iodine K x rays from the NaI(Tl) crystal, and the distribution (c) which was obtained without the 1-mm aluminum absorber shows the additional peak produced by the L x rays from gold. For all angles in the coincidence measurements, the window of the pulse height selector was adjusted for each target to accept the total distribution of pulses produced by the K x rays from tin and from gold (including the iodine escape peak but not the L x ray peak) as shown in Fig. 3(a) and (b).

For the experimental conditions described above, we

can define the following quantities:

N_K = Coincidence counting rate produced by *true events* in which the γ detector (Fig. 1) receives a photon incoherently scattered by a K -shell electron at the same time as the K detector (Fig. 1) receives the accompanying K x ray.

N_F = Counting rate produced in the γ detector (Fig. 1) from photons scattered by electrons *initially free and at rest*.

n_K = Number of K -shell electrons per cm^2 in the target in a plane perpendicular to the incident photon direction.

n_F = Number of electrons per cm^2 *initially free and at rest* in the target in a plane perpendicular to the incident photon direction.

m = Number of photons per second incident on the target.

Ω_k = Solid angle subtended by the γ detector (Fig. 1) from the center of the target.

$\epsilon_{k(F)}$ = Detection efficiency of the γ detector (Fig. 1) for photon scattered in the acceptance solid angle, Ω_k , by electrons *initially free and at rest*.

$\epsilon_{k(K)}$ = Detection efficiency of the γ detector (Fig. 1) for photons incoherently scattered in the acceptance solid angle, Ω_k , by K -shell electrons of a given target.

ϵ_K = Ratio of the number of interactions in the K detector (Fig. 1) produced by K x rays to the total number of K x rays emitted isotropically from the target.

$a_{k(K)}$ = Fraction of photons initially scattered incoherently by K -shell electrons into solid angle Ω_k , and not absorbed by the target.

$a_{k(F)}$ = Fraction of photons initially scattered by free electrons into solid angle Ω_k , and not absorbed by the target.

a_K = Fraction of K x rays initially emitted into the acceptance angle of the K detector (Fig. 1) and not absorbed by the target.

$\bar{\omega}_K$ = Probability that a K x ray will be emitted from the atom when an electron is removed from the shell (K -fluorescent efficiency).

$d\sigma_K$ = Cross section for Compton scattering by K -shell electrons. This cross section is differential with respect to the photon scattering angle, and is integrated over all energies of the scattered photon.

$d\sigma_F$ = Cross section for Compton scattering from electrons *initially free and at rest*. This cross section is differential with respect to the photon scattering angle.

With the above definitions, the differential cross section per unit solid angle for the Compton scattering of 660-keV photons at a given angle by the K -shell electrons of tin and gold, is given by the following equation:

$$d\sigma_K/d\Omega = N_K/mn_Ka_K\bar{\omega}_K\epsilon_K\epsilon_{k(K)}a_{k(K)}\Omega_k. \quad (1)$$

On the other hand, the differential Compton cross

section per unit solid angle for the scattering of 660-keV photons at a given angle by the electrons that are *initially free and at rest* in a target, is given by the following equation:

$$d\sigma_F/d\Omega = N_F/mn_F a_{k(F)} \epsilon_{k(F)} \Omega_k. \quad (2)$$

Then the ratio of the cross sections defined by Eqs. (1) and (2) is given by the following equation:

$$\frac{d\sigma_K}{d\sigma_F} = \left(\frac{N_K}{N_F}\right) \left(\frac{n_F}{n_K}\right) \left(\frac{\epsilon_{k(F)}}{\epsilon_{k(K)} \epsilon_K}\right) \left(\frac{a_{k(F)}}{a_{k(K)} a_K}\right). \quad (3)$$

This method of determining the cross section $d\sigma_K$ in terms of the ratio $d\sigma_K/d\sigma_F$, simplifies the experimental problems and at the same time ties the measurements to the predictions of the well-established Klein-Nishina formula. The procedure for determining the various quantities in Eq. (3) is outlined below, along with estimates of the various systematic errors. The ratio n_F/n_K is readily determined from the information about the targets given below (Secs. 2C and 2E), and is estimated to have an accuracy of better than 5%.

B. True Coincidence Counting Rate

The coincidence counts produced by *true* events must be distinguished from chance coincidence counts and from coincidence counts produced by *false* events. Therefore the true coincidence counting rate N_K for a given angle is given by the following equation:

$$N_K = N_t - N_c - N_f, \quad (4)$$

where N_t is the total coincidence counting rate measured with a given target (tin or gold), N_c is the chance coincidence counting rate, and N_f is the false coincidence counting rate.

The chance rate N_c was measured initially for some cases by the insertion of a 2- μ sec delay line in one detector channel. For the remaining cases, the chance rate was calculated from the usual expression, $2\tau N_1 N_2$, where the counting rate of each channel N_1 and N_2 is of the order of 100 counts per second for all cases. Several measurements were made of the resolving time, τ , which was found to be consistently equal to 5.3×10^{-7} sec.

Two possible sources for false coincidence counts are (a) secondary production of K x rays in the target by recoil electrons, and (b) secondary scattering of the photons into one detector from the other detector or from the surrounding material. (A third source of false coincidence counts is the double Compton effect which is expected to be small and which is corrected for by the aluminum target procedure described below.) In the present measurement, source (a) was mostly eliminated by the use of thin targets in which multiple scattering effects are negligible (see Sec. E). To minimize the contribution of false counts from source (b), very little material was left in the vicinity of the target, and shield-

ing was placed around the detectors to limit their field of view to the region in the vicinity of the target. The contribution of the false coincidence counts was experimentally determined by a procedure in which the high- Z target was replaced by an equivalent aluminum foil with the same number of electrons per cm^2 . Then the false coincidence counting rate N_f is approximately equal to the coincidence counting rate measured with the aluminum target minus the corresponding chance coincidence counting rate.

The above procedure for estimating the false counting rate by the substitution of an equivalent aluminum foil does not exactly reproduce the scattering effects that occur with the given high- Z targets. The two main differences are that the scattering effects of the K x-rays from the high- Z targets are not reproduced with the aluminum target and the coherent scattering at small angles is negligible for the aluminum compared to the high- Z targets. However, the scattering effects introduced by the K x rays are expected to be small because of the large photoelectric cross section. In addition such effects were reduced in the present measurements because pulses with amplitudes corresponding to photon energies less than approximately 100 keV were rejected by the pulse height selector of the γ detector (Fig. 1). Coherent scattering effects for these conditions become appreciable for scattering angles less than 20 degrees. Precautions were taken to minimize this effect at the small angles by increasing the shielding between the two detectors and restricting the field of view of the K detector so that there was no unshielded path between the two open faces of the crystals. The validity of this substitution method was checked by varying the shielding and scattering conditions with different sizes and positions for the shielding materials; in all of these cases, the same value within the experimental error was obtained for the true coincidence counting rate N_K . On the basis of the above tests the aluminum substitution method was estimated to give the false coincidence counting rate with an accuracy better than 5%.

C. Counting Rate for Compton Scattering by Free Electrons

The counting rate N_F applies only to the photons that are scattered from the target into the γ detector (Fig. 1) by electrons *initially free and at rest*. Therefore, it is desirable to measure this quantity with a low- Z target in which the electron binding energies and the small-angle coherent scattering of the photons are both negligible. An aluminum target was used in the present measurements to satisfy the above criteria. (The binding energies of the K and L shell electrons in aluminum are approximately 1.6 and 0.08 keV, respectively.⁷) For a given scattering angle, N_F is equal to the difference in the counting rates of the γ detector with and without the target in the photon beam. In order to minimize any

uncertainties due to the target thickness, background fluctuations, or absorption effects, measurements were made with aluminum targets of different thicknesses. The quantity N_F was found to be directly proportional to the target thickness with no indication of any spurious effects. From the thickness curve, the value of N_F at a given angle was selected for an aluminum target with a thickness equal to 0.27 g/cm². The values obtained for N_F by this procedure are estimated to have an accuracy of better than 2%. As a final check, the value of N_F divided by the solid angle Ω_K was plotted for the different scattering angles, and the shape of this curve showed good agreement with the cross-section curve predicted by the Klein-Nishina formula for 660-keV photons.

D. Detector Efficiency

The efficiency, ϵ_K , of the K detector (Fig. 1) was determined from the data of Wolicki *et al.*⁸ who calculated crystal efficiencies on the basis of known absorption coefficients for different geometries and photon energies. These data were applied to the target-detector distances in Table I. In addition, a small correction was made for the absorption of the K x rays in the crystal windows described in Sec. 2A. According to the above procedure, the values obtained for the efficiency ϵ_K are 0.075 and 0.080 at a distance of 0.75 in. and 0.019 and 0.20 at a distance of 1.75 in., for the K x rays from gold and tin, respectively. The above estimates require that all of the interactions in the crystal for the K x rays from tin and gold produce pulses that are accepted by the window of the pulse height selector for the K detector (see discussion in Sec. 2A). As a check on these efficiency values, the total number of K x rays emitted isotropically from the gold target was measured with a collimated 2-in. diam, 2-in. long NaI(Tl) crystal which detected all of the incident x rays with a 100% efficiency. (This collimated large crystal was not used for the coincidence measurements because the geometry would require a large reduction in the solid angles and therefore in the counting rates.) The total number of K x rays measured with the small and the large crystal on the basis of the above efficiencies agreed within a few percent.

The efficiency ratio $\epsilon_{k(F)}/\epsilon_{k(K)}$ applies to the γ detector (Fig. 1) for photons scattered from the target, which has a $\frac{3}{4}$ -in. diam lead collimator and a 1-in. diam 1-in. thick NaI(Tl) crystal (density ≈ 3.67 g/cm³). For this detector, the ratio is given by the following equation:

$$\frac{\epsilon_{k(F)}}{\epsilon_{k(K)}} = \frac{A(1 - e^{-0.3 \mu_K})}{B(1 - e^{-0.3 \mu_F})} \quad (5)$$

For the photons incoherently scattered into the γ detector by the *electrons initially free and at rest* or by

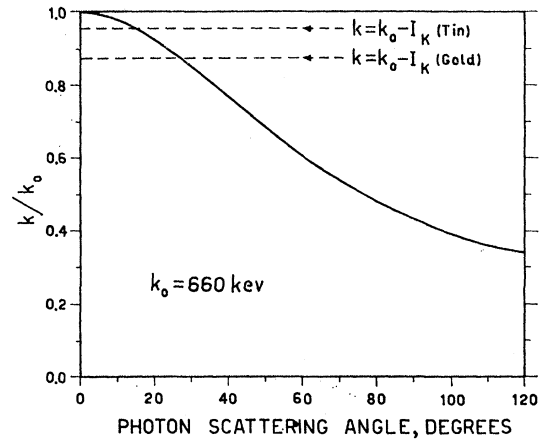


FIG. 4. Angular dependence of the scattered photon energy k for the Compton scattering by electrons initially free and at rest, of photons with an initial energy k_0 of 660 keV. The values of k given by the dashed lines are the maximum energies of the photons incoherently scattered by the K -shell electrons of tin (for which the K -shell binding energy, I_K , is equal to 29.2 keV) and of gold (for which I_K is equal to 80.7 keV).

the K -shell electrons, A or B , respectively, are the fractions of the total number of interactions in the crystal that produce pulses accepted by the window of the pulse height selector, and μ_F or μ_K , respectively, are the absorption coefficients of the NaI(Tl) crystal. The value of μ_F is obtained from the absorption data supplied by Grodstein³ for a given photon energy which is related to the scattering angle as shown by the curve in Fig. 4. On the other hand, the value of μ_K is uncertain because the photons incoherently scattered from the K shell electrons at a given angle have an undetermined distribution of energies. On the basis of the nonrelativistic results of DuMond and his collaborators³ (see Part I), a conservative estimate can be made that most of the photons incoherently scattered by the K -shell electrons are contained in an energy interval of about twice the K -shell binding energy, or about 200 keV (for gold) in the present measurements. Because the absorption coefficient for NaI(Tl) does not change greatly over such an interval, it is reasonable to select the value of μ_K corresponding to an effective photon energy. For angles larger than 20 degrees, this effective photon energy is selected to be approximately equal to the energy for free electron scattering shown in Fig. 4. For 20 degrees where the energy transfer to the free electron is less than the K -shell binding energy for gold as shown in Fig. 4, the effective photon energy for gold was selected to be equal to the maximum energy $k_0 - I_K$, where k_0 is the incident photon energy and I_K is the K -shell binding energy for gold. To cover any uncertainties at the small angles (less than 60 degrees) a systematic error of ± 80 keV (not exceeding the upper limit of $k_0 - I_K$) was assigned to the values of the effective photon energy. Fortunately those errors are less than 10% because of the relatively small variation in the absorption coefficient. To estimate the ratio A/B

⁸ E. A. Wolicki, R. Jastrow, and F. Brooks, Naval Research Laboratory Report ONRL 4833 (unpublished).

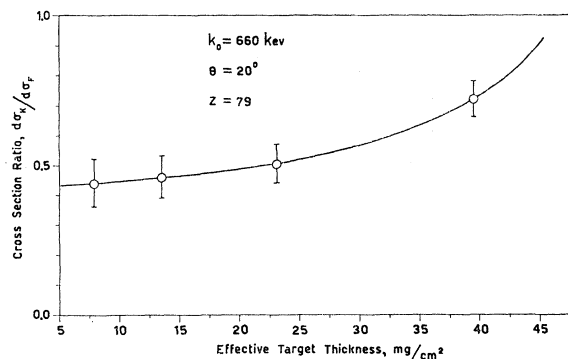


FIG. 5. Dependence of the apparent cross-section ratio $d\sigma_K/d\sigma_F$ on the thickness of the gold target for an incident photon energy of 660 kev. The differential cross sections for Compton scattering by K shell electrons $d\sigma_K$, and by electrons initially free and at rest $d\sigma_F$, are determined from Eq. (3). The effective target thickness is equal to the true thickness divided by $\cos\alpha$, where α is the target inclination angle to the incident photon beam (see Fig. 1).

for different photon energies, plots were made of the fraction F of the total number of pulses accepted by the pulse height selector as a function of the lower discriminator setting of the window. These plots were made for different photon energies on the basis of the pulse height distribution curves shown in Fig. 2. The results obtained from these plots showed that, for the lower discriminator setting of 100 kev used in these measurements (see Sec. 1), the fraction F was approximately constant over the range of photon energies from about 150 to 600 kev, and therefore the ratio A/B is approximately equal to unity. This result simply indicates that the efficiency ratio given by Eq. (5) is not appreciably effected by the fact that the pulse height selector does not accept pulses with amplitudes below a minimum value provided that this value corresponds to a photon energy that is small compared to the energy of the scattered photons. As a check on this condition, measurements were made with minimum pulse amplitudes corresponding to 100 and 150 kev at a scattering angle of 20 degrees and the values obtained for the cross-section ratio in the two cases agreed within a few percent. On the basis of the above conditions, the value of the efficiency ratio $\epsilon_{k(F)}/\epsilon_{k(K)}$ is estimated to be equal to unity for all of the scattering angles with a systematic error of approximately 5%.

E. Target Thickness Corrections

There are two possible effects associated with the finite thickness of the target, that may influence the experimental value for the cross section ratio defined by Eq. (3). First is the secondary production of K x rays in the target by the recoil electrons with energies larger than the K -shell ionization energy. Second is the absorption in the target of the K x rays and of the photons incoherently scattered by either the free electrons or the K -shell electrons. If the target is thin enough, both of

these effects have a negligible influence on the cross-section ratio.

In the present experiment, the cross-section ratio was measured for different thicknesses of both the gold and the tin targets. The results obtained for the gold targets are shown in Fig. 5, where the cross section ratio was determined from Eq. (3), and the *effective target thickness*, T , is equal to the target thickness divided by $\cos\alpha$ (see Fig. 1). The curve in Fig. 5 shows that the target thickness effects for gold are negligible for values of T less than approximately 15 mg/cm². Similarly it was found that the target thickness effects for tin are negligible for values of T less than approximately 10 mg/cm². For the final coincidence measurements, the target thicknesses were selected to be 7.5 mg/cm² (with $\alpha=0^\circ$) for tin and 6.7 mg/cm² (with $\alpha=60^\circ$) for gold. The fact that the cross section ratio for these targets is independent of the target thickness automatically requires the ratio of the absorption corrections $a_{k(F)}/a_{k(K)}$ to be equal to unity. Also, only a few percent of the total number of K x rays emitted from the gold or the tin atoms are absorbed in these thin targets. Estimates for a_K were made from the known absorption coefficients for an average target thickness calculated for the target detector geometry shown in Fig. 1, where α is equal to 60 degrees for gold and zero degrees for tin. The values obtained for a_K are 0.99 for the gold target and 0.97 for the tin target.

F. K-Shell Fluorescent Yields for Tin and Gold

The K -shell fluorescent yield, $\bar{\omega}_K$, has been experimentally determined for most of the elements by many

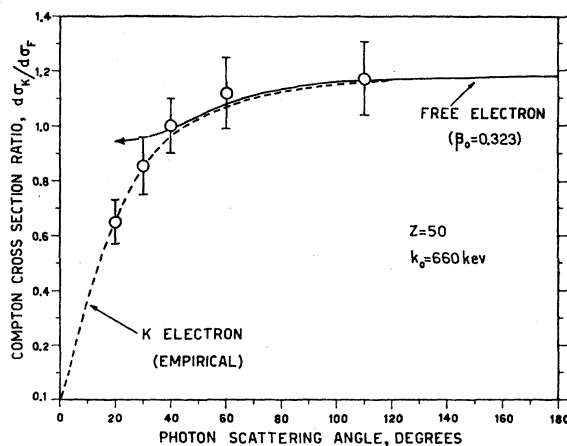


FIG. 6. Angular dependence of the cross-section ratio $d\sigma_K/d\sigma_F$ for an incident photon energy of 660 kev. The cross section $d\sigma_K$ is the Compton cross section for a K -shell electron of tin and $d\sigma_F$ is equal to the Klein-Nishina cross section for an electron initially free and at rest. The experimental results are determined from Eq. (3) and are given by the open circles and the dashed line. The theoretical curve given by the solid line represents a large angle approximation with $d\sigma_K$ equal to the Compton cross section $(d\sigma)_{av}$ [defined by Eq. (10)] for an electron initially free but with a velocity ($\beta_0=0.323$) corresponding to the K -shell binding energy of tin.

investigators. On the basis of these studies, Wapstra *et al.*⁹ have prepared tabulated values of $\bar{\omega}_K$ as a function of the atomic number, and the errors are estimated to be less than 2%. Within these error limits, the values for $\bar{\omega}_K$ for the targets in the present measurements, are found from the above data to be

$$\begin{aligned}\bar{\omega}_K &= 0.84 & \text{for } Z=50 \text{ (tin),} \\ \bar{\omega}_K &= 0.95 & \text{for } Z=79 \text{ (gold).}\end{aligned}$$

3. RESULTS AND DISCUSSION

A summary of the experimental data obtained in these measurements is presented in Table I. This table gives the coincidence counting rates for 7.5-mg/cm² tin target and for the 6.7-mg/cm² gold target at scattering angles of 20, 30, 40, 60, and 110 degrees. The false coincidence counting rate was measured with an aluminum target having the same number of electrons per cm² as the corresponding tin or gold target. Only the statistical errors for the counting rates are given in this table.

The cross section ratio $d\sigma_K/d\sigma_F$ given by Eq. (3), was evaluated with the data in Table I and with the information given in Sec. 2. The experimental values for this cross-section ratio are shown by the open circles

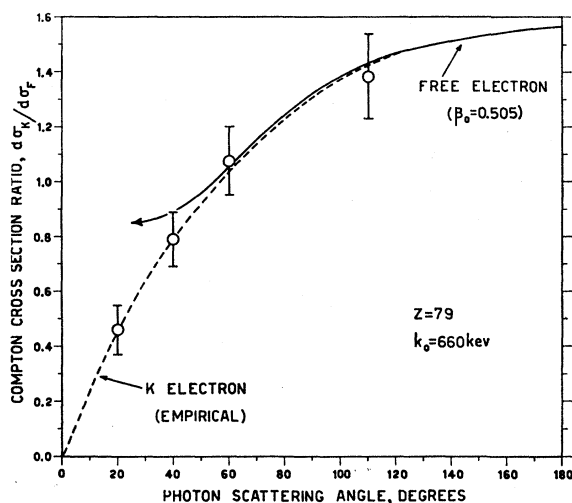


FIG. 7. Angular dependence of the cross-section ratio, $d\sigma_K/d\sigma_F$, for an incident photon energy, k_0 , of 660 keV. The cross section $d\sigma_K$ is the Compton cross section for a K-shell electron of gold, and $d\sigma_F$ is equal to the Klein-Nishina cross section for an electron initially free and at rest. The experimental results are determined from Eq. (3) and are given by the open circles and the dashed line. The theoretical curve given by the solid line represents a large-angle approximation with $d\sigma_K$ equal to the Compton cross section ($d\sigma_{av}$ [defined by Eq. (10)] for an electron initially free with a velocity ($\beta_0=0.505$) corresponding to the K-shell binding energy of gold.

⁹ A. H. Wapstra, G. I. Nijgh, and R. Van Lieshout, *Nuclear Spectroscopy Tables* (North-Holland Publishing Company, Amsterdam, 1959), p. 82.

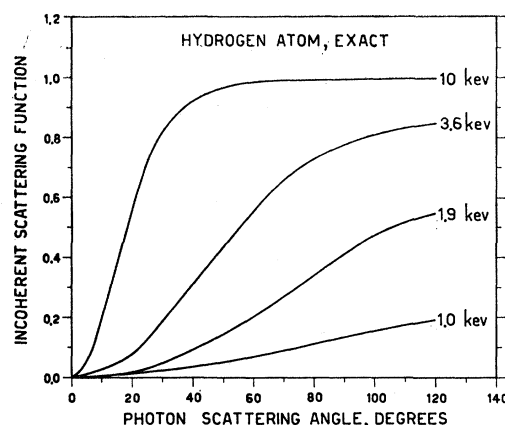


FIG. 8. Angular dependence of the incoherent scattering function⁸ calculated for the hydrogen atom (0.0136-keV electron binding energy), for incident photon energies of 1.0, 1.9, 3.6, and 10 keV.

for tin and gold in Figs. 6 and 7, respectively. The dashed curves in these figures are based on the experimental points, and show the approximate experimental dependence of the cross-section ratio on the photon scattering angle.

The experimental curves in Figs. 6 and 7 show that for small scattering angles, the cross-section ratio is less than unity and approaches zero as the angle decreases to zero. This behavior simply indicates that at the small scattering angles, the momentum transfer to the K-shell electrons tends to be small compared with their initial momentum, and there is a small probability that the atom will absorb enough energy to remove the electron from the K shell. A similar behavior for this ratio is predicted by the nonrelativistic calculations of the incoherent scattering function discussed by Grodstein.⁸ For example, the incoherent scattering function for the hydrogen atom has been calculated analytically,⁸ and the dependence of this function on the photon scattering angle is shown in Fig. 8 for incident photon energies of 1.0, 1.9, 3.6, and 10 keV. These nonrelativistic theoretical results show that the function (which is equal⁸ to the cross-section ratio $d\sigma_K/d\sigma_F$) approaches zero at the small scattering angles, and for a given scattering angle the function decreases as the ratio of the incident photon energy to the K shell binding energy decreases. The same type of behavior is found in the experimental results where for example at 20 degrees, the cross-section ratio is less for the K electrons of gold than for the K electrons of tin. Unfortunately no relativistic calculations are available that can be directly compared with these experimental results at small angles. The behavior of $d\sigma_K$ in Figs. 6 and 7 disagrees with the results obtained by Brini *et al.*⁵ (This disagreement is not surprising in view of the fact that the results by the aforementioned authors did not contain corrections for the contribution of false coincidence counts and target thickness effects.)

An interesting situation occurs at the large scattering angles. In this region, the energy transfer to the K -shell electrons is large compared with their initial energy, and therefore the K -shell electrons may be considered to be *free* but *not at rest*. Accordingly at large angles, the cross section for scattering by the K -shell electrons approaches the Compton cross section for scattering by *free* electrons *with velocities equal to the velocities of the K -shell electrons*. Here it is important to point out that the Compton cross section, which is differential with respect to the photon scattering angle, depends on the reference system selected for the electron. Therefore the Compton cross section for scattering by K -shell electrons can be expected to have an angular dependence at large angles that is different than the predictions of the Klein-Nishina formula¹ which is derived in the electron rest system.

For a reference system where the initial electron velocity is not zero, the cross section formula for Compton scattering by free electrons, which is differential with respect to the photon scattering angles θ , is given by Jauch and Rohrlich¹⁰ as

$$\frac{d\sigma}{d\Omega} = \frac{r_0^2}{2} \frac{(1-\beta_0^2)}{(1-\beta_0 \cos\alpha)^2} \left(\frac{k}{k_0}\right)^2 \bar{X}, \quad (6)$$

where the classical electron radius r_0 is equal to approximately 2.82×10^{-13} cm, β_0 is the ratio of the incident electron velocity to the velocity of light, α is the angle between the incident electron and photon, and k_0 is the incident photon energy. The energy of the scattered photon, k , is given as

$$k = \frac{k_0(1-\beta_0 \cos\alpha)}{1 + (k_0/E_0)(1-\cos\theta) - \beta_0 \cos\alpha}, \quad (7)$$

where E_0 is the total energy (including the rest energy) of the incident electron. The quantity \bar{X} is defined by the equation

$$\bar{X} = \frac{K}{K'} + \frac{K'}{K} + 2\left(\frac{1}{K} - \frac{1}{K'}\right) + \left(\frac{1}{K} - \frac{1}{K'}\right)^2, \quad (8)$$

where

$$\begin{aligned} K &= E_0 k_0 (1 - \beta_0 \cos\alpha), \\ K' &= E_0 k_0 (1 - \beta_0 \cos\alpha) + k_0 k (\cos\theta - 1). \end{aligned} \quad (9)$$

The cross section $d\sigma$, which is defined by Eq. (6), can be used to estimate the large-angle Compton scattering by K -shell electrons in the following manner. As a first

¹⁰ J. M. Jauch and F. Rohrlich, *The Theory of Protons and Electrons* (Addison-Wesley Publishing Company, Inc., Cambridge, Massachusetts, 1955), p. 232. This formula is given by Eq. (11-17) which is summed over the photon polarizations by replacing X with \bar{X} defined in Eq. (11-14).

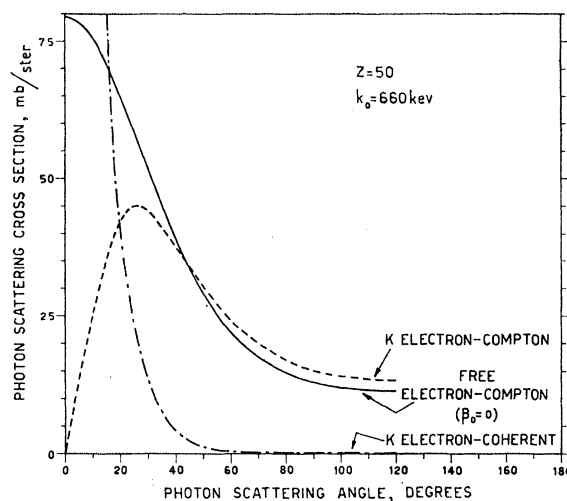


Fig. 9. Comparison of the cross sections for the scattering of 660-keV photons by free electrons and by the K -shell electrons of tin. The cross section for Compton scattering by an electron initially free and at rest is obtained from the Klein-Nishina formula and is shown by the solid line. The cross section for Compton scattering by a K -shell electron of tin is obtained from the experimental results in Fig. 6 and is shown by the dashed line. The cross section for coherent scattering by a K -shell electron of tin is predicted by the calculations of Brown and Mayers¹¹ and is shown by the dot-dashed line.

approximation for large-angle scattering, the K -shell electron may be considered to be free and to have a single value for its velocity corresponding to the K -shell binding energy. Because all values of α are equally probable for K -shell scattering, it is necessary to calculate an average cross section. In an exact calculation, the scattering amplitudes are averaged over α . However, for the present case where the photon wavelength is not large compared to the K -shell Bohr radius, interference effects may be neglected, and as an approximate procedure it is sufficient to average the cross section $d\sigma$ over α . Then the expression for this average cross section $\langle d\sigma/d\Omega \rangle_{av}$ is given as

$$\left\langle \frac{d\sigma}{d\Omega} \right\rangle_{av} = \int_1^{-1} \left(\frac{d\sigma}{d\Omega} \right) d(\cos\alpha) / \int_1^{-1} d(\cos\alpha). \quad (10)$$

This integration was carried out both analytically and graphically for given values of θ . The analytical formula for $\langle d\sigma/d\Omega \rangle_{av}$ is rather lengthy and is not reproduced here. However $\langle d\sigma \rangle_{av}$ was evaluated for the conditions of this experiment where the initial photon energy is 660 keV and the initial electron kinetic energy is equal to the K -shell binding energy for tin (29.2 keV)⁷ and gold (80.7 keV).⁷ For comparison, the Klein-Nishina cross section $d\sigma_F$ was evaluated for the same experimental conditions. The dependence of this theoretical cross-section ratio $\langle d\sigma \rangle_{av}/d\sigma_F$ on the photon scattering angle is shown by the solid line for tin in Fig. 6 and for gold in Fig. 7. The results show that at large angles, the cross-section ratio is greater than unity for high- Z

atoms, and approaches unity as the K -shell binding energy (or the electron velocity) decreases to zero. The experimental curves given by the dashed lines for gold and tin show good agreement at large angles with this estimated cross-section ratio.

As the photon scattering angle decreases to zero, the decrease in the cross section for Compton scattering by K -shell electrons is accompanied by an increase in the cross section for coherent scattering. A comparison of these two cross section with the Klein-Nishina cross section for electrons initially free and at rest is shown in Fig. 9 for tin and Fig. 10 for gold. In these figures the angular dependence of the coherent cross section for one K electron is obtained from the results of Brown and Mayers¹¹ and includes a correction of approximately 25% for the contribution of L -shell and Thomson scattering. The dashed lines show the experimental Compton cross section for the K -shell electrons obtained by the product of the experimental cross-section ratio given in Figs. 6 and 7 with the Klein-Nishina cross section $d\sigma_F$. The importance of electron binding effects in the scattering of 660-keV photons is indicated in Figs. 9 and 10 by a comparison of the combined coherent and Compton cross section for the K -shell electron with the Klein-Nishina cross section for the free electron.

A comparison of the total Compton cross section for 660-keV photons scattered by K -shell electrons σ_K , and

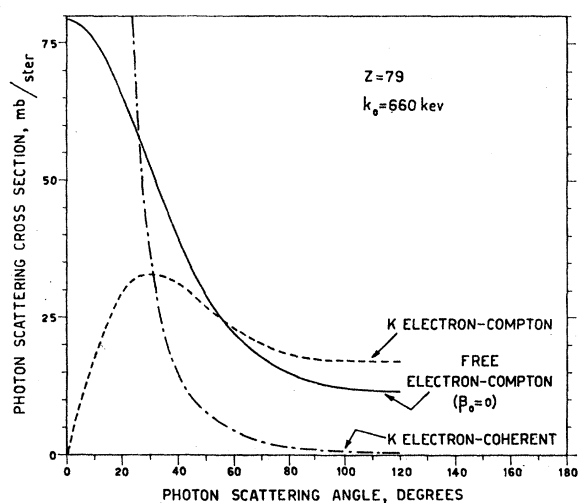


FIG. 10. Comparison of the cross sections for the scattering for 660-keV photons by free electrons and by the K -shell electrons of gold. The cross section for Compton scattering by an electron initially free and at rest is obtained from the Klein-Nishina formula and is shown by the solid line. The cross section for Compton scattering by a K -shell electron of gold is obtained from the experimental results in Fig. 7 and is shown by the dashed line. The cross section for coherent scattering by a K -shell electron of gold is predicted by the calculations of Brown and Mayers¹¹ and is shown by the dot-dashed line.

¹¹ G. E. Brown and D. F. Mayers, Proc. Roy. Soc. (London) A242, 89 (1957).

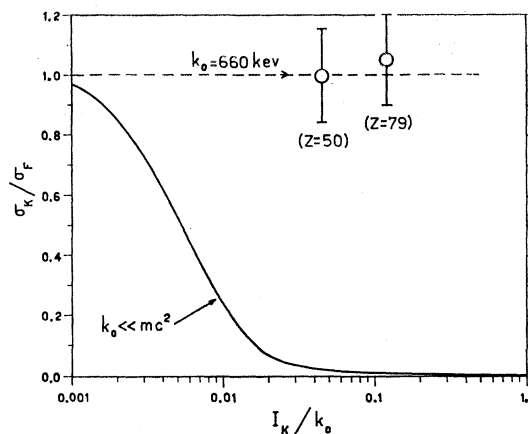


FIG. 11. Dependence of the integrated Compton cross-section ratio, σ_K/σ_F , on the ratio of the K -shell binding energy, I_K , to the incident photon energy, k_0 . The cross section σ_K is the total Compton cross section (integrated over the photon scattering angle) for a K -shell electron, and σ_F is the total Klein-Nishina cross section (integrated over the photon scattering angle). The theoretical solid curve applies to non-relativistic photon energies, and was derived from the curves in Fig. 8 which give the incoherent scattering function for the hydrogen atom. The experimental values of the total Compton cross ratio σ_K/σ_F for tin ($I_K=29.2$ kev)⁷ and gold ($I_K=80.7$ kev)⁷, with k_0 equal to 660 kev, are given by the open circles and the estimated empirical curve is given by the dashed line.

by electrons σ_F initially free and at rest, can be made by integrating the differential cross sections $d\sigma_K$ (dashed curve) and $d\sigma_F$ (solid curve), in Figs. 9 and 10, over all of the photon scattering angles. The total cross-section ratio σ_K/σ_F is plotted in Fig. 11 as a function of the energy ratio, I_K/k_0 , where I_K is the binding energy for a K -shell electron and k_0 is the energy of the incident photon. The experimental values of this cross-section ratio for tin and gold are given by the open circles and the dashed line is an estimated empirical curve. This cross-section ratio is equal to unity and zero when I_K is equal to zero and k_0 , respectively. For comparison the theoretical cross-section for non-relativistic photon energies, $k_0 \ll mc^2$, was obtained from the curves in Fig. 8. For each photon energy in Fig. 8, the differential Compton cross section for the electron in the hydrogen atom, $d\sigma_K$, is given³ by the product of the incoherent scattering function and the Klein-Nishina cross section $d\sigma_F$. Then $d\sigma_K$ and $d\sigma_F$ are integrated over all of the photon scattering angles to give the total Compton cross section σ_K and σ_F for initial photon energies of 1.0, 1.9, 3.6, and 10 kev. The resulting ratio, σ_K/σ_F , for these non-relativistic photon energies is plotted as a function of I_K/k_0 (where the binding energy of the electron in the hydrogen atom is equal to approximately 0.0136 kev⁷) and is shown by the solid line in Fig. 11. The solid curve in Fig. 11 for non-relativistic photon energies indicates an appreciable decrease in the total Compton cross section for relatively small electron binding energies. For example for a value of I_K/k_0 equal to 0.01, the cross-section ratio decreases from unity to

approximately 0.25. On the other hand, for 660-kev photons, the total Compton cross section appears to be independent of the electron binding energy. It is interesting to note that at 660 kev, the small- and large-angle behavior of $d\sigma_K$ has a compensating effect in which the total cross-section ratio, σ_K/σ_F , is approximately equal to unity for both tin and gold.

ACKNOWLEDGMENTS

We wish to thank Professor Marc Ross for helpful discussions. Also one of us (JWM) wishes to thank Professor Mario Ageno for his suggestions during the course of the work and for his kind hospitality in making available the facilities of the Physics Laboratory of the Istituto Superiore di Sanita.

PHYSICAL REVIEW

VOLUME 124, NUMBER 5

DECEMBER 1, 1961

Electron Scattering from Hydrogen*

CHARLES SCHWARTZ

Department of Physics, University of California, Berkeley, California

(Received June 12, 1961)

Kohn's variational principle has been used to calculate S -wave elastic scattering of electrons from atomic hydrogen, using up to 50 trial functions of the type introduced by Hylleraas to describe the bound states of two-electron atoms. The phase shifts calculated at several energies up to 10 ev appear to have converged well, leaving residual uncertainties mostly less than one thousandth of a radian. Taking extra pains to include the effect of the long-range force at zero energy, we have also determined very accurate values for the scattering lengths.

INTRODUCTION

THE scattering of electrons from hydrogen atoms has been the subject of a great many calculations since it presents what is probably the simplest non-trivial real problem in scattering theory. We undertook a program of computing definitive values of the S -wave elastic phase shifts for this system, making no approximations other than those imposed by the finite speed and capacity of modern computing machines. Our use of the variational method¹ for this scattering problem completes, in a sense, the famous work on the bound states of two-electron atoms begun more than thirty years ago by Hylleraas.

Probably the most interesting, and quite unexpected, result of this program has been the realization of the extraordinary nature of the convergence of the "stationary" phase shift. It has been recognized for some time² that, in contrast with bound-state problems, the addition of more variational parameters in a scattering calculation does not necessarily lead to a better answer. This behavior is blamed on the nonexistence of any minimum (or maximum) principle. The error in a variational calculation may be represented by

$$\int \Delta(E-H)\Delta d\tau \quad (1)$$

* Supported in part by the Advanced Research Projects Administration through the U. S. Office of Naval Research.

¹ A calculation identical to ours but limited to zero energy and using only a small number of parameters has recently been reported by Y. Hara, T. Ohmura, and T. Yamanouchi, *Progr. Theoret. Phys. (Kyoto)* **25**, 467 (1961).

² See, for example, H. S. W. Massey in *Handbuch der Physik* edited by S. Flügge (Springer-Verlag, Berlin, 1956), Vol. 36.

where Δ is the unknown error in the trial wave function. Only for systems where one knows the (finite) number of eigenvalues of H below the value E can one possibly state that the expression (1) must be negative.³ For scattering at any finite energy it is clearly impossible to make any such statement. We have discussed elsewhere⁴ how, by taking a great deal of numerical data, one can draw smooth curves and see an effectively regular convergence for the general scattering problem at any energy. This paper will present the results of this treatment for the e - H problem.

We use Kohn's variational principle,

$$[\tan\delta/k] = \tan\delta/k + (2m/\hbar^2) \int \psi(E-H)\psi d\tau_1 d\tau_2, \quad (2)$$

where

$$(2m/\hbar^2)(E-H) = k^2 - 1 + \nabla_1^2 + \nabla_2^2 + (2/r_1) + (2/r_2) - (2/r_{12}),$$

with lengths in units of \hbar^2/me^2 ; and our trial wave function is (for singlet or triplet states) $\psi = \varphi + \chi$,

$$\varphi = (1 \pm P_{12})2e^{-r_2}[\sin kr_1/kr_1 + \tan\delta \cos kr_1/kr_1(1 - e^{-(\kappa/2)r_1})]/4\pi\sqrt{2}, \quad (3a)$$

$$\chi = \sum_{l,m,n \geq 0} C_{lmn} e^{-(\kappa/2)(r_1+r_2)} r_{12}^l \times (r_1^m r_2^n \pm r_1^n r_2^m)/4\pi\sqrt{2}, \quad (3b)$$

³ L. Rosenberg, L. Spruch, and T. F. O'Malley, *Phys. Rev.* **119**, 164 (1960), have in this manner established minimum principles for scattering at zero energy. These authors have recently extended their method to positive energies, but only by mutilating the potentials.

⁴ C. Schwartz, *Ann. Phys.* (to be published).